Hindawi
Advances in Civil Engineering
Volume 2019, Article ID 7168703, 9 pages
https://doi.org/10.1155/2019/7168703

Research Article

Optimization of the Mixture Design of Low-CO_2 High-Strength Concrete Containing Silica Fume

Seung-Jun Kwon [1] **and Xiao-Yong Wang** [2]

[1]*Department of Civil and Environmental Engineering, Hannam University, Daejeon-Si, Republic of Korea*
[2]*Department of Architectural Engineering, Kangwon National University, Chuncheon-Si, Republic of Korea*

Correspondence should be addressed to Xiao-Yong Wang; wxbrave@kangwon.ac.kr

Received 15 March 2019; Accepted 23 May 2019; Published 11 June 2019

Guest Editor: Endong Wang

As abundant CO_2 is released by high-strength concrete due to its high binder content, the reduction of CO_2 emissions has become increasingly important. This study proposed a general procedure to optimize the mixture design of low-CO_2 high-strength concrete containing silica fume. First, the equations for evaluating strength and slump were regressed based on available experimental results. CO_2 emissions were calculated based on the concrete mixtures and the unit CO_2 emissions of the concrete components. By using the genetic algorithm, the concrete mixtures with the lowest CO_2 emissions were determined by considering various constraints. Second, the cost of concrete was calculated based on the concrete mixtures and the unit cost of the concrete components. Similarly, the concrete mixtures with the lowest cost were determined based on the genetic algorithm. We found that, in some cases, the mixtures with the lowest CO_2 emissions were different from those with the lowest cost. Third, through adding the constraint equation of cost, Pareto optimal mixtures with relatively lower CO_2 emissions and lower cost were determined. In summary, the proposed technique is valuable for designing high-strength concrete considering both CO_2 emissions and cost.

1. Introduction

High-strength concrete is increasingly used in the modern construction industry. Many advantages can be achieved by using high-strength concrete such as reducing the quantity of sections needed in structural elements, increasing the occupancy rate of buildings, and extending the service life of the building [1]. However, high-strength concrete generally has a lower water-to-binder ratio than normal strength concrete. As abundant binder is used and lots of CO_2 is released when producing high-strength concrete, the reduction of CO_2 emissions has become more and more important [2].

Fundamental studies have been conducted regarding the evaluation of CO_2 emissions of high-strength concrete. Larsen et al. [3] found that ultra-high-performance concrete could offer increased benefits over traditional concrete design. Voo and Foster [4] and Yu et al. [5] proposed that using slag in producing ultra-high-performance concrete could reduce CO_2 emissions and embodied energy and save total life cycle cost. Park et al. [6] assessed the life cycle CO_2 emissions of concrete with different strength levels and found that life cycle CO_2 increased linearly as the compressive strength increased. Kim et al. [7] proposed a method for evaluating CO_2 emissions from the production process of concrete and found that the application of high-strength concrete and the standardization of the mixing process could reduce CO_2 emissions in the construction stage. Latawiec et al. [8] proposed an index for concrete desirability where the effects of compressive strength, durability, CO_2 emissions, and cost on concrete desirability were considered.

On the other hand, some methods have been proposed for the material design of low-CO_2 or low-cost concrete. Based on neural networks and the genetic algorithm, Yeh [9] proposed software for designing concrete mixtures with the

lowest possible cost. Mosaberpanah and Eren [10] proposed a full factorial method to maximize the strength and minimize the carbon dioxide emissions. The effects of cement content, silica fume content, fiber content, water-to-binder ratio, and superplasticizer are considered for determining strength and CO_2 emissions. Yang et al. [11] proposed an approach for designing low-CO_2 concrete containing various supplementary cementitious materials such as fly ash, slag, and silica fume. Tapali et al. [12] proposed an iteration approach to design concrete with a low environmental cost, considering strength and service life. Khan et al. [13] designed low-cost high-strength self-compacting concrete using a response surface methodology. The optimal combinations of cement, water-to-binder ratio, fine aggregate, fly ash, and superplasticizer were determined using a desirability function. Ji et al. [14] combined neural networks and a harmony search algorithm to find the optimal design of reactive powder concrete with the lowest cost. Although many studies [9–14] have been carried out on the design of low-CO_2 or low-cost concrete, some questions need to be further clarified: first, what are the differences between the mixture designs of low-CO_2 concrete and low-cost concrete? Second, how can we design concrete with both low CO_2 emissions and low cost? Third, how can we create a general design procedure of low-CO_2 concrete for different countries whose design codes may be different?

In this study, we proposed a general procedure to optimize the mixture design of low-CO_2 high-strength concrete containing silica fume. By using the genetic algorithm, concrete mixtures with the lowest CO_2 emissions and lowest cost were individually determined. We found that, for some cases, the mixtures with the lowest CO_2 emissions were different from those with the lowest cost. Furthermore, through adding the constraint equation of cost, Pareto optimal mixtures with relatively lower CO_2 emissions and lower cost were determined.

The innovations of this study are summarized as follows: first, we propose a general method for designing low-CO_2 concrete; second, we consider the difference between low-CO_2 concrete and low-cost concrete; third, we propose a Pareto optimal method to determine mixtures with lower CO_2 and lower cost.

2. Optimization Design of Concrete Mix Proportions

To optimize the mixing proportions of high-strength concrete containing silica fume, the object function and constraint conditions need to be established. In this study, the CO_2 emissions were placed as the object function. The constraint conditions were the desired concrete strength, workability, component contents, component ratios, and absolute volume [9].

2.1. Object Function. The total CO_2 emissions of silica fume-blended concrete include CO_2 emissions from the concrete materials and transport and from the mixing of the concrete [15]. The total CO_2 emissions can be calculated from the following equation [15]:

$$CO_{2-e} = CO_{2-eM} + CO_{2-eT} + CO_{2-eP} \quad (1)$$

where CO_{2-e}, CO_{2-eM}, CO_{2-eT}, and CO_{2-eP} represent the total CO_2 emissions, CO_2 emissions from concrete materials, CO_2 emissions from transport, and CO_2 emissions from the mixing operation of concrete, respectively. CO_{2-eM} can be calculated according to the concrete mixture and unit CO_2 emissions of the concrete components as follows:

$$\begin{aligned} CO_{2-eM} = {} & CO_{2-C} * C + CO_{2-SF} * SF + CO_{2-W} * W \\ & + CO_{2-CA} * CA + CO_{2-S} * S + CO_{2-SP} * SP \end{aligned} \quad (2)$$

where CO_{2-C}, CO_{2-SF}, CO_{2-W}, CO_{2-CA}, CO_{2-S}, and CO_{2-SP} are the unit CO_2 emissions of cement, silica fume, water, coarse aggregate, sand, and superplasticizer, respectively, and C, SF, W, CA, S, and SP are the masses of cement, silica fume, water, coarse aggregate, sand, and superplasticizer in the concrete mixtures, respectively. Table 1 shows the CO_2 emissions of the concrete components [11]. In this study, the object function was placed as CO_{2-eM}.

2.2. Constraint Conditions. The object function (the minimum CO_2 emission, CO_{2-eM}) is exposed to various constraints, for example, concrete strength, workability, component contents, component ratios, and absolute volume [9].

The strength constraint means that the design strength should be higher than the required strength. The formula for the strength constraint is shown as follows [9]:

$$f_c(t) \geq f_{cr}(t), \quad t = 3, 7, 28, \ldots, \text{days}, \quad (3)$$

where $f_c(t)$ is the concrete strength at age t and $f_{cr}(t)$ is the required strength at age t.

The workability constraint of fresh concrete is shown in the following equation [9]:

$$\text{Slump} \geq \text{Slump}^r, \quad (4)$$

where Slump^r is the required slump of concrete.

The range of component contents is shown as follows:

$$\text{lower} \leq \text{component} \leq \text{upper}, \quad (5)$$

where the components are the cement, silica fume, binder, water, fine aggregate, coarse aggregate, and superplasticizer. Table 2 shows the lower and upper limits of the contents of concrete components [16].

The component ratio constraint is shown as follows:

$$R_l \leq R_i \leq R_u, \quad (6)$$

where R_i is the component ratio (for example, the water-to-binder ratio, water-to-cement ratio, sand ratio, silica fume-to-binder ratio, and superplasticizer-to-binder ratio). R_l and R_u are the lower and upper limits of the component ratio, respectively. Table 3 shows the component ratio constraints [16]. Because the aim of this study is to design silica fume-blended concrete with high strength, the range of binder

Table 1: Unit CO_2 emissions of the concrete components [11].

Cement (kg/kg)	Silica fume (kg/kg)	Water (kg/kg)	Fine aggregate (kg/kg)	Coarse aggregate (kg/kg)	Superplasticizer (kg/kg)
0.931	1.05	0.000196	0.0026	0.0075	0.25

Table 2: Constraints of the contents of concrete components.

	Cement (kg/m^3)	Silica fume (kg/m^3)	Binder (cement + silica fume) (kg/m^3)	Water (kg/m^3)	Fine aggregate (kg/m^3)	Coarse aggregate (kg/m^3)
Lower limit	450	25	574	140	500	700
Upper limit	710	210	833	165	900	1050

Table 3: Constraints of the ratios of concrete components.

	Water-to-binder ratio	Water-to-cement ratio	Sand ratio	Silica fume-to-binder ratio	Superplasticizer-to-binder ratio
Lower limit	0.18	0.211	0.35	0.05	0.0188
Upper limit	0.27	0.317	0.39	0.25	0.0469

content is higher and the range of water-to-binder ratio is lower than those of ordinary strength concrete [9].

The absolute volume constraint is shown as follows:

$$\frac{W}{\rho_W} + \frac{C}{\rho_C} + \frac{SF}{\rho_{SF}} + \frac{S}{\rho_S} + \frac{CA}{\rho_{CA}} + \frac{SP}{\rho_{SP}} + V_{air} = 1, \quad (7)$$

where ρ_W, ρ_C, ρ_{SF}, ρ_S, ρ_{CA}, and ρ_{SP} are the densities of water, cement, silica fume, sand, coarse aggregate, and superplasticizer, respectively, and V_{air} is the volume of air in the concrete. The densities of water, cement, silica fume, sand, coarse aggregate, and superplasticizer are 1000, 3150, 2260, 2610, 2700, and 1220 kg/m^3, respectively. Equation (7) implies that the sum of each concrete component should equal 1 m^3 [9].

2.3. Property Evaluation of the Silica Fume-Blended Concrete. Lim et al. [16] conducted experimental studies on the strength and slump of silica fume-blended high-strength concrete where a total of 77 mixing proportions of concrete were studied. The effects of the water-to-binder ratio, water content, sand ratio, silica fume replacement ratio, and superplasticizer content on the mechanical workability of concrete were considered [16]. The compressive strength of high-strength concrete at 28 days ranged from 90 to 120 MPa. The slump of concrete ranged between 180 and 235 mm. The upper and lower limits of contents of concrete components are shown in Table 2. The upper and lower limits of the ratios of concrete components are shown in Table 3. Based on the experimental results of compressive strength [16], the strength of concrete at 28 days can be regressed as a function of the water-to-binder ratio, water content, sand ratio, and silica fume replacement ratio. The regression equation of compressive strength is shown as follows:

$$f_c = -182.90\frac{W}{C+SF} - 0.51 * W + 117.15\frac{S}{S+CA} + 49.49\frac{SF}{C+SF} + 170.17. \quad (8)$$

First, equation (8) shows that as the water content and water-to-binder ratio increases, concrete strength decreases. This is due to the increase in the porosity of the concrete. Next, as the sand ratio increases, the strength of the concrete increases. This is because when compared with coarse aggregate, the range of the interfacial transition zone of fine aggregate is not obvious [17]. Third, as the silica fume replacement ratio increases, the concrete strength increases. This is because the pozzolanic reaction of silica fume can produce secondary calcium silicate hydrate and improve the concrete strength. The correlation index between the experimental results and the regression results of compressive strength was 0.954. The high correlation index proves the validity of equation (8).

Based on the experimental results of slump [16], the slump of concrete can be regressed as a function of the water-to-binder ratio, water content, sand ratio, silica fume replacement ratio, and superplasticizer content. The regression equation of slump is shown as follows:

$$\text{slump} = 209.27 * \frac{W}{C+SF} + 1.33 * W - 325.10\frac{S}{S+CA} - 69.28 * \frac{SF}{C+SF} + 1.28 * SP + 63.30. \quad (9)$$

As shown in this equation, as the water content, superplasticizer content, and water-to-binder ratio increase, the concrete slump increases. As the sand ratio and silica fume replacement ratio increase, the concrete slump decreases.

Based on the mixtures of concrete, the superplasticizer content is determined as a function of the water-to-binder ratio and the silica fume replacement ratio [16]. The regression equation of superplasticizer content is shown as follows:

$$SP = 47.34 - 142.46\frac{W}{C+SF} + 28.77\frac{SF}{C+SF}. \quad (10)$$

As shown in this equation, as the water-to-binder ratio decreases or the silica fume replacement ratio increases, the superplasticizer content increases [18].

Summarily, within this section, we determined the object function and constraints of the concrete mixing proportions. The object function was the minimum CO_2 emissions, CO_{2-eM}. The constraints included various mechanical and constructability performance measures, for example, the compressive strength, workability of fresh concrete, component contents, component ratios, and absolute volume of the concrete mixture. Once the object's function and constraints are solved, concrete mixtures that meet various performance requirements can be acquired.

On the other hand, it should be noticed that the equations for evaluating strength, slump, and superplasticizer content are obtained from materials mixed by Lim et al. [16]. For other countries, because the compositions of binders and the varieties of superplasticizer may be different from Lim et al. [16], the calculation equations of strength, slump, and superplasticizer may also be different from those proposed in this study.

The technique for solving the object's function with constraints is the genetic algorithm. The genetic algorithm is an adaptive global optimization probability search algorithm that simulates the genetic and evolutionary processes of living things in the natural environment [19]. The process of the genetic algorithm is summarized as follows: Step 1: generate the initial population; Step 2: calculate the fitness; Step 3: select cross mutation operations, and compute fitness function; Step 4: check convergence criteria; and Step 5: repeat Step 3 until the convergence criteria are met.

In this study, we used the MATLAB global optimization toolbox for solving objective optimization with constraints [19]. The object function and constraints equation can be set in the MATLAB global optimization toolbox. According to the genetic algorithm, the optimal mixture which has the minimum CO_2 emission and can meet various constraints can be found.

3. Illustrative Examples

3.1. Design of Low-CO_2 High-Strength Concrete. In this section, examples are shown for the mixture design of low-CO_2 high-strength concrete with different strength levels such as 95, 100, 105, 110, and 115 MPa. The required slump was assumed to be 180 mm. The air content was assumed to be 2%. The object function of the genetic algorithm was the minimum CO_2 emission.

The strength of concrete can be evaluated using equation (8), the slump of concrete can be evaluated using equation (9), and CO_2 emissions can be evaluated using the unit CO_2 emission (Table 1) and concrete mixtures. The constraints included the range of the concrete components, range of the component ratios, and absolute volume. Based on the genetic algorithm that considers the various constraints, the mixtures were calculated and are shown in Table 4. The strengths of Mix1, Mix2, Mix3, Mix4, and Mix5 were 95, 100, 105, 110, and 115 MPa, respectively. The following results were obtained based on the contents of Table 4. First, as the required strength of concrete increased, the silica fume contents in the mixtures also increased. This shows the significance of silica fume in producing high-strength concrete. Second, the water contents for concrete with higher strengths, such as Mix3 (105 MPa), Mix4 (110 MPa), and Mix5 (115 MPa), were equal to the lower limit of water (Table 2). This means that a lower water content is helpful for producing high-strength concrete.

The performances of Mixes 1–5 are shown in Table 5. The following results were obtained based on the contents of Table 5. First, as the compressive strength of concrete increased from 95 MPa to 115 MPa, the water-to-binder ratio decreased from 0.26 to 0.23 and the silica fume replacement ratio increased from 0.05 to 0.25. This means that a lower water-to-binder ratio and a higher silica fume replacement ratio can improve the strength of concrete. Second, the sand ratio for each mixture was equal to the upper limit of the sand ratio (Table 3). This is because the concrete strength increases as the sand ratio increases (equation (8)). Third, the slumps for each mixture were all higher than the required slump of 180 mm. As the strength of the concrete increased, the superplasticizer content also increased. Fourth, as shown in Figure 1(a), as the strength of concrete increased, the CO_2 emissions also increased. Furthermore, based on the unit cost of concrete components (Table 6 [9]) and concrete mixtures, the cost for each mixture was calculated and they are shown in Figure 1(b). As the strength of concrete increased, the cost for each mixture also increased.

3.2. Design of Low-Cost High-Strength Concrete. In Section 3.1, the objective function of the genetic optimization was set as the minimum CO_2 emissions. However, in the concrete industry, concrete producers and construction companies are interested not only in CO_2 emissions but also in the cost of concrete. Like CO_2 emissions, the cost of concrete can also be calculated from the contents and unit prices of the concrete components (Table 6 [9]).

Based on similar methods in Section 3.1, the concrete mixture with the lowest price, considering various constraint equations, can be determined. The mixtures were calculated and are shown in Table 7. The strengths of Mix6, Mix7, Mix8, Mix9, and Mix10 were 95, 100, 105, 110, and 115 MPa, respectively. The following results were obtained based on the contents of Tables 7 and 8. First, for concrete with strengths of 95 and 100 MPa, the mixtures of the lowest cost were the same as that of the lowest CO_2 emissions (Mix1 was the same as Mix6 and Mix2 was the same as Mix7). For the concrete with strengths of 95 MPa and 100 MPa, the silica fume replacement ratio was 0.05, which equaled the lower limit of the silica fume replacement ratio (Table 3). Second, for concrete with strengths of 105, 110, and 115 MPa, the silica fume replacement ratio of the lowest cost mixtures (Mix8, Mix9, and Mix10) was lower than that of the lowest CO_2 emission mixtures (Mix3, Mix4, and Mix5). For example, the compressive strengths of Mix3 and Mix8 were both 105 MPa, but the silica fume replacement ratio of Mix8 was lower than that of Mix3. This is because the unit price of silica fume is much higher than that of cement (the unit price

Table 4: Mixtures of low-CO_2 high-strength concrete.

Low-CO_2 concrete	Cement (kg/m^3)	Silica fume (kg/m^3)	Water (kg/m^3)	Fine aggregate (kg/m^3)	Coarse aggregate (kg/m^3)	Superplasticizer (kg/m^3)
Mix1-95 MPa	545.30	28.70	149.62	659.81	1032.01	11.65
Mix2-100 MPa	545.30	28.70	143.55	664.83	1039.86	13.15
Mix3-105 MPa	521.27	52.73	140.00	663.62	1037.97	15.24
Mix4-110 MPa	463.29	110.71	140.00	653.61	1022.32	18.14
Mix5-115 MPa	452.54	150.85	140.00	635.86	994.56	21.48

Table 5: Performance of low-CO_2 high-strength concrete.

Low-CO_2 concrete	f_c (MPa)	Slump (mm)	CO_2 emission (kg/m^3)	Cost (NT dollar/m^3)	Water/binder	Silica fume/binder	Sand ratio	Sp/binder
Mix1-95 MPa	95.00	202.79	550.21	2271.93	0.26	0.05	0.39	0.02
Mix2-100 MPa	100.00	194.40	550.65	2312.92	0.25	0.05	0.39	0.02
Mix3-105 MPa	105.00	188.14	554.02	2580.69	0.24	0.09	0.39	0.03
Mix4-110 MPa	110.00	184.89	561.50	3169.04	0.24	0.19	0.39	0.03
Mix5-115 MPa	115.00	182.74	594.22	3668.59	0.23	0.25	0.39	0.04

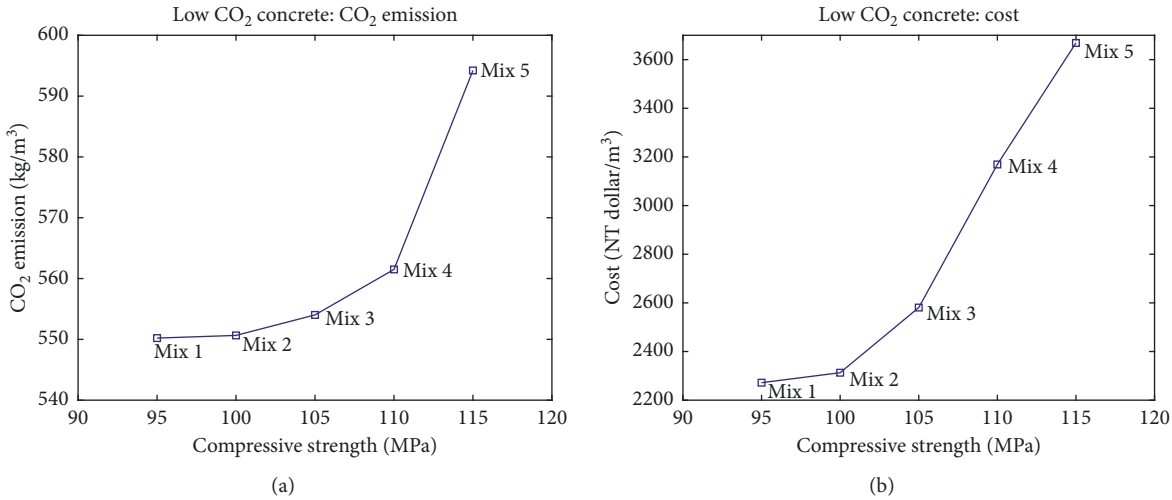

Figure 1: (a) CO_2 emissions of low-CO_2 concrete. (b) Cost of low-CO_2 concrete.

Table 6: Unit cost of the concrete components [9].

Cement (NT dollar/kg)	Silica fume (NT dollar/kg)	Water (NT dollar/kg)	Fine aggregate (NT dollar/kg)	Coarse aggregate (NT dollar/kg)	Superplasticizer (NT dollar/kg)
2.25	11.25	0.01	0.28	0.236	25.1

Table 7: Mixtures of low-cost high-strength concrete.

Low-cost concrete	Cement (kg/m^3)	Silica fume (kg/m^3)	Water (kg/m^3)	Fine aggregate (kg/m^3)	Coarse aggregate (kg/m^3)	Superplasticizer (kg/m^3)
Mix6-95 MPa	545.30	28.70	149.62	659.81	1032.01	11.65
Mix7-100 MPa	545.30	28.70	143.55	664.83	1039.86	13.15
Mix8-105 MPa	571.86	30.10	140.00	656.99	1027.60	15.65
Mix9-110 MPa	648.03	34.11	140.00	626.71	980.23	19.54
Mix10-115 MPa	663.51	71.13	140.00	601.65	941.05	22.98

Table 8: Performance of low-cost high-strength concrete.

Low-cost concrete	f_c (MPa)	Slump (mm)	Cost (NT dollar/m^3)	CO_2 emission (kg/m^3)	Water/binder	Silica fume/binder	Sand ratio	Sp/binder
Mix6-95 MPa	95.00	202.79	2271.93	550.21	0.26	0.05	0.39	0.02
Mix7-100 MPa	100.00	194.40	2312.92	550.65	0.25	0.05	0.39	0.02
Mix8-105 MPa	105.00	189.20	2445.90	577.36	0.23	0.05	0.39	0.03
Mix9-110 MPa	110.00	188.50	2740.48	653.02	0.21	0.05	0.39	0.03
Mix10-115 MPa	115.00	186.61	3261.80	706.80	0.19	0.10	0.39	0.03

of silica fume is five times that of cement (Table 6)). When the object function is the lowest price, the content of silica fume will be as low as possible. Third, for concrete with strengths of 105 MPa, 110 MPa, and 115 MPa, the water-to-binder ratio of the lowest cost mixtures (Mix8, Mix9, and Mix10) was lower than that of the lowest CO_2 emission mixtures (Mix3, Mix4, and Mix5). This means that a lower water-to-binder ratio can compensate for the impairment of strength due to the lower silica fume content. Fourth, the slumps for each mixture were all higher than the required slump of 180 mm. As the strength of concrete increased, the superplasticizer content also increased. Fifth, as shown in Figure 2(a), as the strength of concrete increased, the cost of concrete also increased. As shown in Figure 2(b), as the strength of concrete increased, the CO_2 emissions for each mixture also increased.

3.3. Pareto Optimal Mixtures for Lower CO_2 Emissions and Lower Cost. As shown in Sections 3.1 and 3.2, for concrete with higher strengths such as 105, 110, and 115 MPa, the mixtures with the lowest cost were different from those with the lowest CO_2 emissions. Although the aims of the lowest CO_2 emissions and lowest price cannot be achieved simultaneously, some compromises can be made between low CO_2 emissions and low price. In other words, we can design concrete with relatively lower CO_2 emissions at a relatively lower price. To design concrete with both lower cost and lower CO_2 emissions, we set an additional constraint regarding the cost of concrete. For example, when the required strength of concrete is given as 110 MPa (the strengths of Mix4 and Mix9 were both 110 MPa), the constraint equation of cost can be set as follows:

$$\text{COST} = (2800, 2900, 3000, 3100). \quad (11)$$

The values of cost (2800, 2900, 3000, and 3100) were between the cost of Mix4 and Mix9 (the cost of Mix4 and Mix9 was 3169.04 and 2740.48, respectively).

The design requirements can be summarized as follows: the object function was the lowest CO_2 emission; the cost of each mixture was equal to 2800 or 2900 or 3000 or 3100, respectively; the design value of compressive strength was 110 MPa; the design value of the slump was 180 mm; and the air content was 2%. In this section, the additional equality constraint was the cost of concrete (equation (11)), while in Section 3.1, there was no constraint for cost.

Based on the genetic algorithm, the mixtures were calculated and named as Mix11, Mix12, Mix13, and Mix14, respectively (shown in Table 9). The performances of Mix11 to Mix14 are shown in Table 10. The following results were obtained based on the contents of Table 10. First, the compressive strengths of Mix11, Mix12, Mix13, and Mix14 were the same, i.e., 110 MPa, and the slumps of Mix11, Mix12, Mix13, and Mix14 were higher than the required slump of 180 mm. Second, the cost of Mix11, Mix12, Mix13, and Mix14 was 2800, 2900, 3000, and 3100, respectively, and the CO_2 emissions of Mix11, Mix12, Mix13, and Mix14 were 640.46, 619.25, 597.92, and 576.43, respectively. The cost and CO_2 emissions of Mix11, Mix12, Mix13, and Mix14 were generally between Mix4 and Mix9. In other words, Mix11, Mix12, Mix13, and Mix14 had both lower cost and lower CO_2 emissions. Figure 3(a) shows the CO_2 emissions versus the concrete cost. As CO_2 emissions increased, concrete cost decreased.

The Pareto optimality is an ideal state of resource allocation. Given an inherent group of people and assignable resources, if there is a change from one state of assignment to another, at least one person's situation becomes better without making anyone's situation worse; this is the Pareto improved state. Pareto's optimal state is the idea that it is impossible to have more Pareto's improved state; in other words, it is impossible to improve the situation of some people without damaging anyone else [20]. Figure 3(b) shows an illustration of the Pareto optimal solutions [21, 22]. The x-axis and y-axis represent that of function f2 and performance f1, correspondingly. Point A and point B are a pair of points on the Pareto optimal solutions graph. At point A, the value of f1 is greater, while at point B, the value of f2 is greater.

Based on the comparison between Figures 3(a) and 3(b), we found that Mix11, Mix12, Mix13, and Mix14 were the Pareto optimal solutions for designing lower CO_2 emissions and lower concrete cost.

3.4. Generalization of the Proposed Method. In this study, the calculation equations of strength and slump were obtained based on the regression of experimental results in [16]. For different design specifications, the calculation equations of strength and slump may be different from those used in this study [23–25]. In addition, the unit CO_2 emission, unit price, constraints of component range, and component ratio used in this study cannot cover all cases presented in different countries and regions [26]. In Sections 3.1–3.3, the air content of concrete is assumed as 2%. The additional mixture designs are performed for different-strength concrete with 1% air content. The analysis results show that when air content changes from 2% to 1%, the contents of cement, silica fume, water, and sand ratio of optimized mixtures do

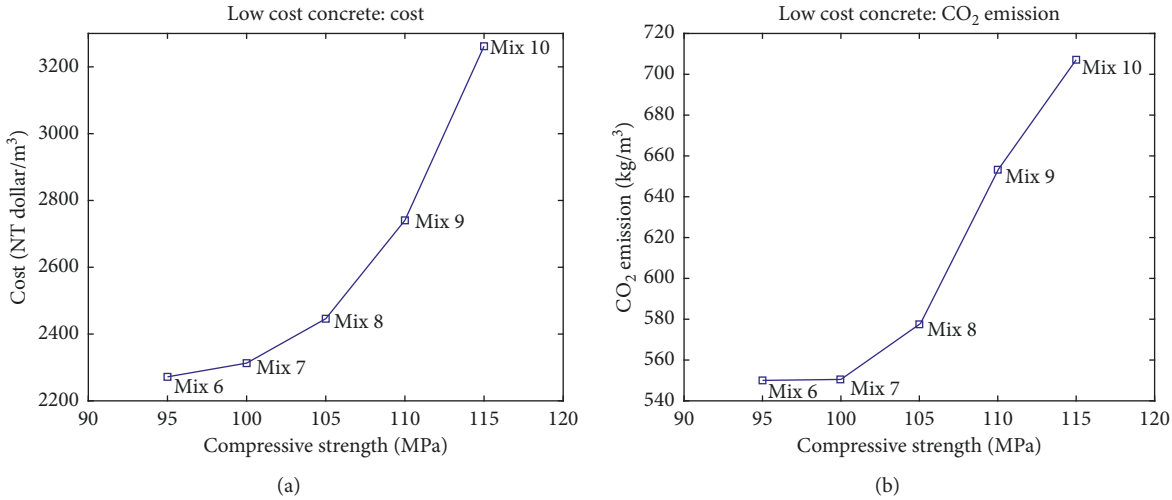

Figure 2: (a) Cost of low-cost concrete. (b) CO_2 emissions of low-cost concrete.

Table 9: Mixtures of 110 MPa concrete with lower CO_2 emissions and lower cost.

Low-CO_2 and cost concrete	Cement (kg/m^3)	Silica fume (kg/m^3)	Water (kg/m^3)	Fine aggregate (kg/m^3)	Coarse aggregate (kg/m^3)	Superplasticizer (kg/m^3)
Mix11-110 MPa	622.65	44.63	140.00	630.38	985.98	19.38
Mix12-110 MPa	579.84	62.38	140.00	636.59	995.69	19.08
Mix13-110 MPa	536.78	80.24	140.00	642.86	1005.50	18.76
Mix14-110 MPa	493.42	98.22	140.00	649.20	1015.41	18.41

Table 10: Performance of 110 MPa concrete with lower CO_2 emissions and lower cost.

Low-CO_2 and cost concrete	Cost (NT dollar/m^3)	CO_2 emissions (kg/m^3)	f_c (MPa)	Slump (mm)	Water/binder	Silica fume/binder	Sand ratio	Sp/binder
Mix11-110 MPa	2800.00	640.46	110.00	188.07	0.21	0.07	0.39	0.03
Mix12-110 MPa	2900.00	619.25	110.00	187.31	0.22	0.10	0.39	0.03
Mix13-110 MPa	3000.00	597.92	110.00	186.48	0.23	0.13	0.39	0.03
Mix14-110 MPa	3100.00	576.43	110.00	185.57	0.24	0.17	0.39	0.03

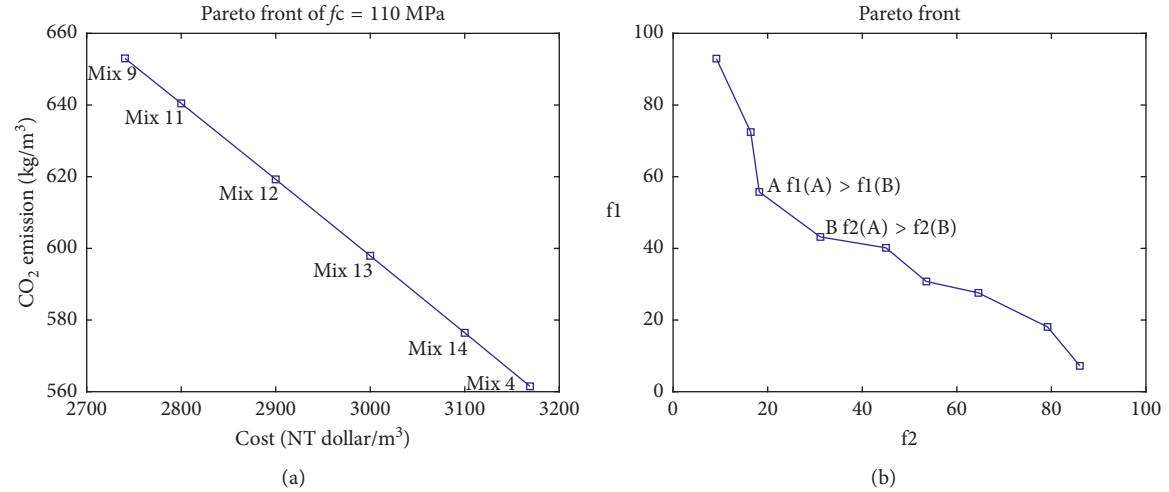

Figure 3: (a) Mixtures for 110 MPa concrete with lower CO_2 emissions and lower cost. (b) Illustration of the Pareto optimal solution.

not change, while the contents of fine aggregate and coarse aggregate increase.

To adapt the proposed design method, other researchers can use their own equations to replace the corresponding equations such as the equations for strength, slump, and various constraints. Although the calculation equations may be different, the basic calculation procedure is very similar. Hence, to some extent the proposed method can be regarded as a general method for the design of low-CO_2 high-strength concrete. On the other hand, as this study focused on the mixture design of high-strength concrete, durability aspects such as carbonation or chloride ingress were not considered. These durability aspects can be considered as additional inequality constraints of the concrete mixture [27].

4. Conclusions

This study proposed a general procedure to optimize the mixture design of low-CO_2 high-strength concrete containing silica fume.

First, CO_2 emissions were calculated based on the concrete mixtures and the unit CO_2 emissions of the concrete components. By using the genetic algorithm, concrete mixtures with the lowest CO_2 emissions were determined considering the various constraints. Similarly, concrete mixtures with the lowest cost were determined based on the genetic algorithm. We found that for concrete with design strengths higher than 105 MPa, the mixtures with the lowest CO_2 emissions were different from those with the lowest cost. As the strength of concrete increased, the CO_2 emissions and cost of concrete also increased.

Second, for concrete with design strength higher than 105 MPa, the objects of the lowest CO_2 emissions and lowest cost cannot be achieved simultaneously. By adding a constraint equation of cost, Pareto optimal mixtures were determined. The Pareto optimal mixtures had relatively lower CO_2 emissions and lower cost. Regarding the Pareto optimal mixtures, as CO_2 emissions increased, the concrete cost decreased. The cost and CO_2 emissions of the Pareto optimal mixtures were between the lowest cost mixture and lowest CO_2 emissions mixture.

In conclusion, the proposed technique is valuable for designing high-strength concrete that considers both CO_2 emissions and cost. To adapt the proposed design method, other researchers can use their own equations to replace the corresponding equations in this study.

Data Availability

The data used to support the findings of this study are available from the corresponding author upon request.

Conflicts of Interest

The authors declare that they have no conflicts of interest.

Acknowledgments

This research was supported by the Basic Science Research Program through the National Research Foundation of Korea (NRF) funded by the Ministry of Science, ICT & Future Planning (No. 2015R1A5A1037548), and a NRF grant (NRF-2017R1C1B1010076).

References

[1] V. G. Papadakis, "Effect of supplementary cementing materials on concrete resistance against carbonation and chloride ingress," *Cement and Concrete Research*, vol. 30, no. 2, pp. 291–299, 2000.

[2] P. K. Mehta, "Reducing the environmental impact of concrete," *Concrete International*, vol. 23, pp. 61–66, 2001.

[3] I. L. Larsen, I. G. Aasbakken, R. O. Born, K. Vertes, and R. T. Thorstensen, "Determining the environmental benefits of ultra high performance concrete as a bridge construction material," *IOP Conference Series: Materials Science and Engineering*, vol. 245, article 052096, 2017.

[4] Y. L. Voo and S. J. Foster, "Characteristics of ultra-high performance "ductile" concrete and its impact on sustainable construction," *IES Journal Part A: Civil & Structural Engineering*, vol. 3, no. 3, pp. 168–187, 2010.

[5] R. Yu, P. Spiesz, and H. J. H. Brouwers, "Development of an eco-friendly ultra-high performance concrete (UHPC) with efficient cement and mineral admixtures uses," *Cement and Concrete Composites*, vol. 55, pp. 383–394, 2015.

[6] J. Park, S. Tae, and T. Kim, "Life cycle CO_2 assessment of concrete by compressive strength on construction site in Korea," *Renewable and Sustainable Energy Reviews*, vol. 16, no. 5, pp. 2940–2946, 2012.

[7] T. Kim, C. Chae, G. Kim, and H. Jang, "Analysis of CO_2 emission characteristics of concrete used at construction sites," *Sustainability*, vol. 8, no. 4, pp. 348–362, 2016.

[8] R. Latawiec, P. Woyciechowski, and K. J. Kowalski, "Sustainable concrete performance—CO_2-emission," *Environments*, vol. 5, no. 2, pp. 27–41, 2018.

[9] I.-C. Yeh, "Computer-aided design for optimum concrete mixtures," *Cement and Concrete Composites*, vol. 29, no. 3, pp. 193–202, 2007.

[10] M. A. Mosaberpanah and O. Eren, "CO_2-full factorial optimization of an ultra-high performance concrete mix design," *European Journal of Environmental and Civil Engineering*, vol. 22, no. 4, pp. 450–463, 2018.

[11] K. H. Yang, S. H. Tae, and D. U. Choi, "Mixture proportioning approach for low-CO_2 concrete using supplementary cementitious materials," *ACI Materials Journal*, vol. 113, no. 4, pp. 533–542, 2016.

[12] J. G. Tapali, S. Demis, and V. G. Papadakis, "Sustainable concrete mix design for a target strength and service life," *Computers and Concrete*, vol. 12, no. 6, pp. 755–774, 2013.

[13] A. Khan, J. Do, and D. Kim, "Cost effective optimal mix proportioning of high strength self compacting concrete using response surface methodology," *Computers and Concrete*, vol. 17, no. 5, pp. 629–638, 2016.

[14] T. Ji, Y. Yang, M. Y. Fu, B. C. Chen, and H. C. Wu, "Optimum design of reactive powder concrete mixture proportion based on artificial neural and harmony search algorithm," *ACI Materials Journal*, vol. 114, no. 1, pp. 41–47, 2017.

[15] H.-S. Lee and X.-Y. Wang, "Evaluation of the carbon dioxide uptake of slag-blended concrete structures, considering the effect of carbonation," *Sustainability*, vol. 8, no. 4, pp. 312–330, 2016.

[16] C.-H. Lim, Y.-S. Yoon, and J.-H. Kim, "Genetic algorithm in mix proportioning of high-performance concrete," *Cement and Concrete Research*, vol. 34, no. 3, pp. 409–420, 2004.

[17] Z. Wu, C. Shi, K. H. Khayat, and S. Wan, "Effects of different nanomaterials on hardening and performance of ultra-high strength concrete (UHSC)," *Cement and Concrete Composites*, vol. 70, pp. 24–34, 2016.

[18] C. Shi, D. Wang, L. Wu, and Z. Wu, "The hydration and microstructure of ultra high-strength concrete with cement-silica fume-slag binder," *Cement and Concrete Composites*, vol. 61, pp. 44–52, 2015.

[19] "Mathworks," 2018, http://www.mathworks.com.

[20] T. Noguchi, I. Maruyama, and M. Kanematsu, "Performance based design system for concrete mixture with multi-optimizing genetic algorithm," in *Proceedings of the 11th International Congress on the Chemistry of Cement (ICCC)*, Durban, South Africa, May 2003.

[21] M. A. DeRousseau, J. R. Kasprzyk, and W. V. Srubar III, "Computational design optimization of concrete mixtures: a review," *Cement and Concrete Research*, vol. 109, pp. 42–53, 2018.

[22] V. Yepes, J. V. Martí, T. García-Segura, and F. González-Vidosa, "Heuristics in optimal detailed design of precast road bridges," *Archives of Civil and Mechanical Engineering*, vol. 17, no. 4, pp. 738–749, 2017.

[23] A. Behnood, V. Behnood, M. M. Gharehveran, and K. E. Alyamac, "Prediction of the compressive strength of normal and high-performance concretes using M5P model tree algorithm," *Construction and Building Materials*, vol. 142, pp. 199–207, 2017.

[24] Z. H. Duan, S. C. Kou, and C. S. Poon, "Prediction of compressive strength of recycled aggregate concrete using artificial neural networks," *Construction and Building Materials*, vol. 40, pp. 1200–1206, 2013.

[25] V. Mechtcherine and S. Shyshko, "Simulating the behaviour of fresh concrete with the distinct element method—deriving model parameters related to the yield stress," *Cement and Concrete Composites*, vol. 55, pp. 81–90, 2015.

[26] J.-S. Chou, C.-F. Tsai, A.-D. Pham, and Y.-H. Lu, "Machine learning in concrete strength simulations: multi-nation data analytics," *Construction and Building Materials*, vol. 73, pp. 771–780, 2014.

[27] X. Y. Wang and Y. Luan, "Modeling of hydration, strength development, and optimum combinations of cement-slag-limestone ternary concrete," *International Journal of Concrete Structures and Materials*, vol. 12, no. 1, pp. 1–13, 2018.